

(Received 1 July 2015; accepted 12 October 2016; first published online 1 February 2016)

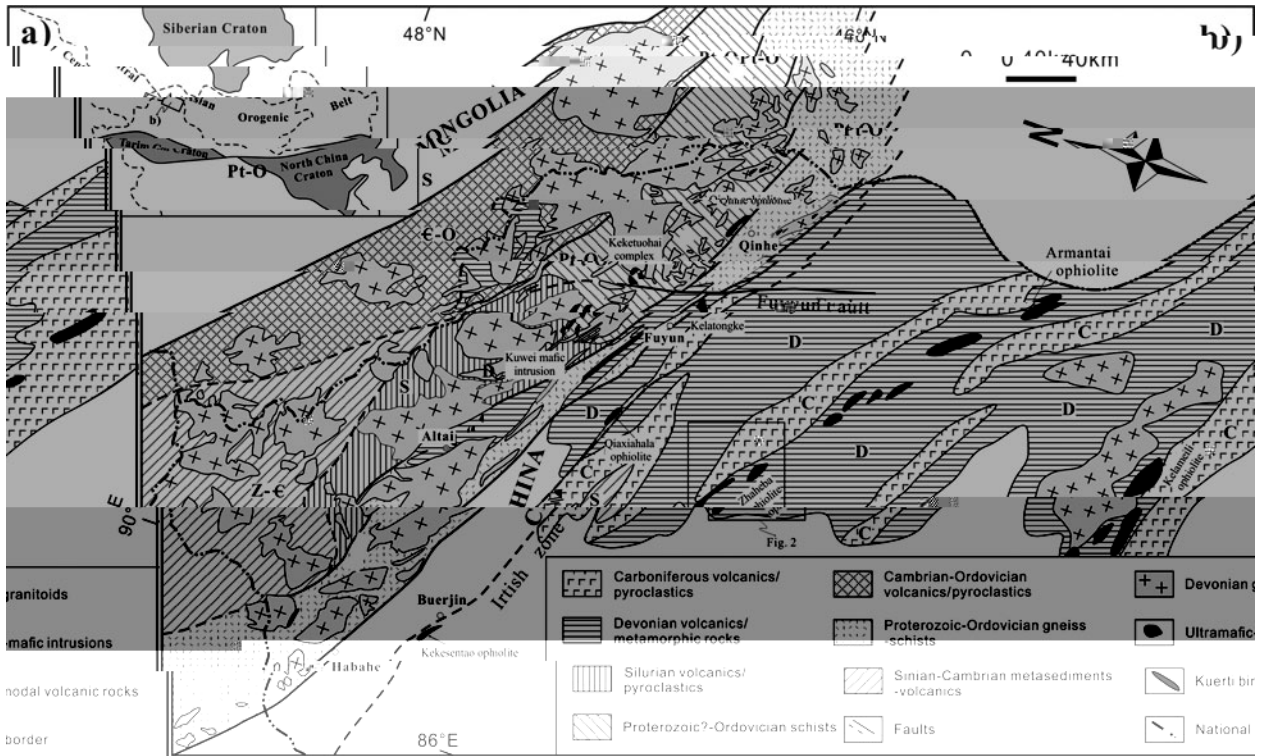
Abstract

The relationship between $\epsilon_v(t)$ (‰) and age (Ma) is shown in Figure 1. The data points are plotted with error bars, showing a general downward trend from approximately 21000 ‰ at 0 Ma to -5305 ‰ at 10000 Ma. A horizontal line is drawn at approximately 10000 ‰. The x-axis ranges from 0 to 10000 Ma, and the y-axis ranges from -5305 to 210016 ‰. The data points are scattered around a central trend line, with some points showing significant deviation. The error bars represent the uncertainty in the measurements. The overall trend suggests a decrease in $\epsilon_v(t)$ over time, which is consistent with the theoretical model proposed in the paper.

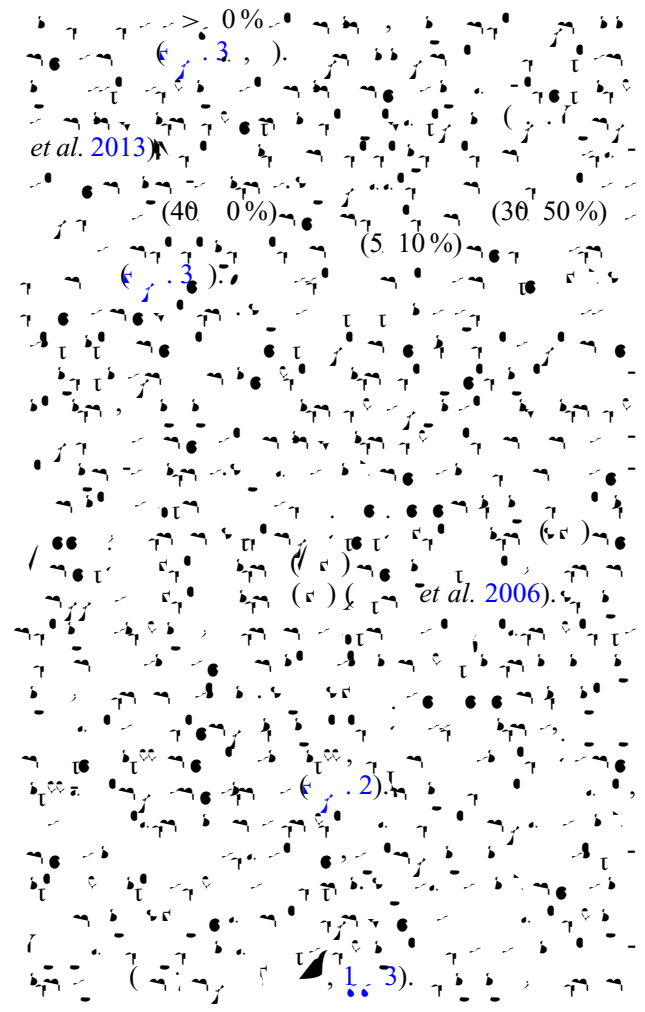
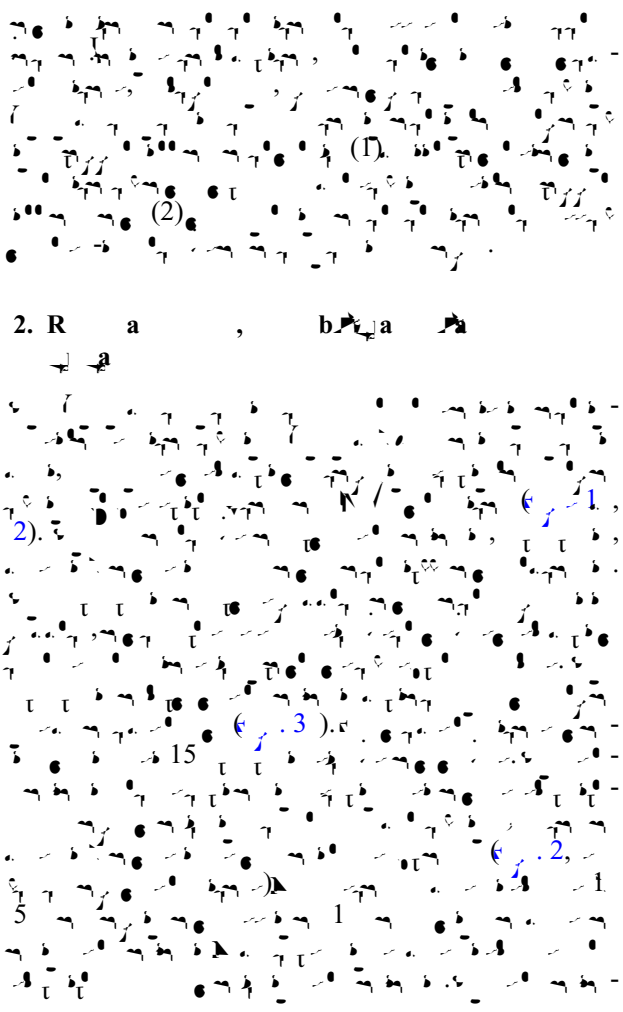
1. Introduction

The relationship between $\epsilon_v(t)$ (‰) and age (Ma) is shown in Figure 1. The data points are plotted with error bars, showing a general downward trend from approximately 21000 ‰ at 0 Ma to -5305 ‰ at 10000 Ma. A horizontal line is drawn at approximately 10000 ‰. The x-axis ranges from 0 to 10000 Ma, and the y-axis ranges from -5305 to 210016 ‰. The data points are scattered around a central trend line, with some points showing significant deviation. The error bars represent the uncertainty in the measurements. The overall trend suggests a decrease in $\epsilon_v(t)$ over time, which is consistent with the theoretical model proposed in the paper.

The relationship between $\epsilon_v(t)$ (‰) and age (Ma) is shown in Figure 1. The data points are plotted with error bars, showing a general downward trend from approximately 21000 ‰ at 0 Ma to -5305 ‰ at 10000 Ma. A horizontal line is drawn at approximately 10000 ‰. The x-axis ranges from 0 to 10000 Ma, and the y-axis ranges from -5305 to 210016 ‰. The data points are scattered around a central trend line, with some points showing significant deviation. The error bars represent the uncertainty in the measurements. The overall trend suggests a decrease in $\epsilon_v(t)$ over time, which is consistent with the theoretical model proposed in the paper.



1. () et al. 200).



2. R a , b a a

et al. 2013) (40 0%) (30 50%) (5 10%) et al. 2006) 1. 3)

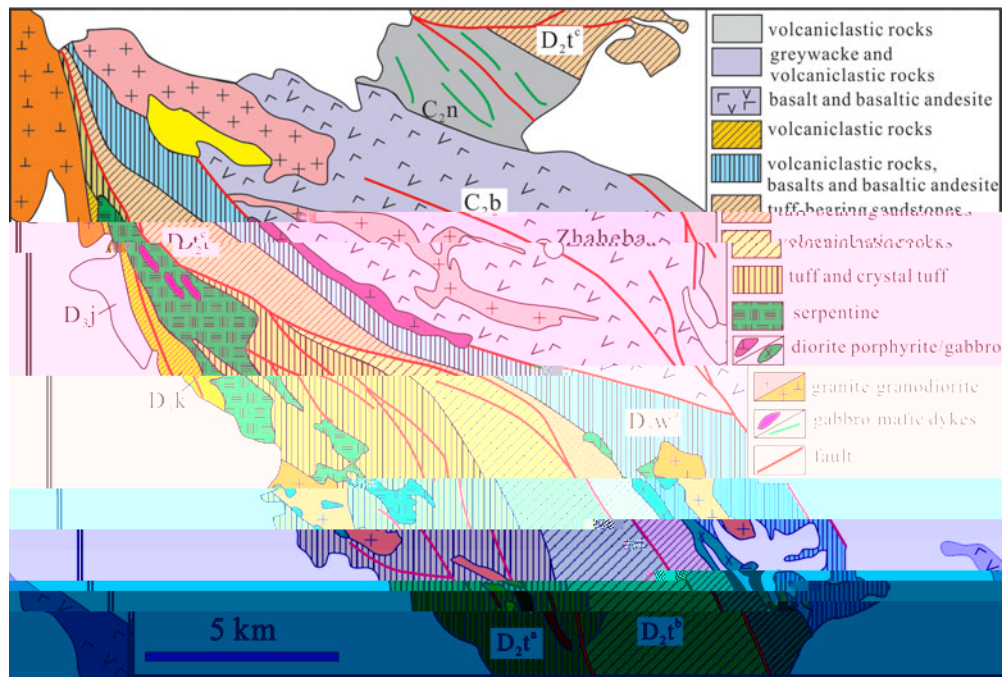


Figure 2. Geological map of the Zhaheba ophiolite (after *et al. 2000, 2001* and *et al. 2003*).

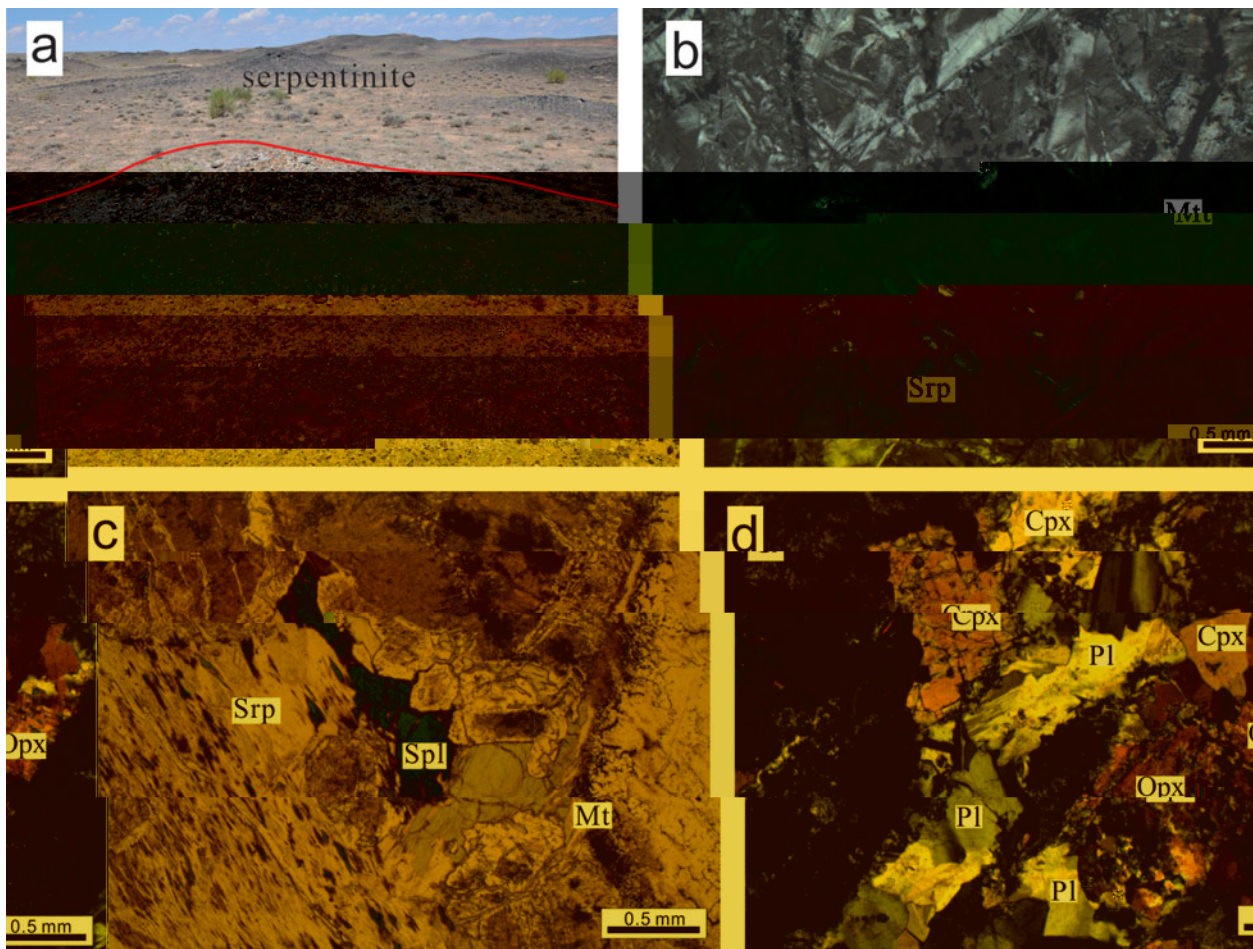


Figure 3. (a) Field photograph of a serpentinite outcrop. (b) Photomicrograph of a mineral assemblage including Magnetite (Mt) and Serpentine (Srp). (c) Photomicrograph showing Serpentine (Srp), Spl, Mt, and Opx. (d) Photomicrograph showing Cpx, Pl, and Onx. Scale bars are 0.5 mm.

3. A a ca

3.a. Z g U Pb a a H O a a

(2013 01, 46° 32' 51" N, 120° 24' 00" E)
(2013 02, 46° 33' 20" N, 120° 23' 36" E)

et al. (2011).

2010)

2003).

et al.

5%

et al. (2010a).

$\frac{^{147}\text{Sm}}{^{143}\text{Nd}} = 0.0020052$,

8% 5.31% (et al. 2010b).

8% $5.44 \pm 0.21\%$ (2),

(et al. 2013).

3.b. M a a a

00
15 15

20
4 5
H

3.c. W a a a

100
et al. (2004).
2%.

6000
et al. (2004).

50

3
-1, -2
-2
3, 3.5%.

1.

et al. (2004).

$\frac{^{147}\text{Sm}}{^{143}\text{Nd}} = 0.114$, $\frac{^{147}\text{Sm}}{^{143}\text{Nd}} = 0.21$,

$\frac{^{147}\text{Sm}}{^{143}\text{Nd}} = 0.102$,

$\frac{^{147}\text{Sm}}{^{143}\text{Nd}} = 0.0506$, $\frac{^{147}\text{Sm}}{^{143}\text{Nd}} = 0.512104$,

$\frac{^{147}\text{Sm}}{^{143}\text{Nd}} = 0.5126$ 1. 2.

4. A a ca

4.a. Z g U Pb a

100, 150 μ
1 1, 2 1.

(et al. 2004).

(22 123) (

5) / 0.4

0. 30.

4 5. ± 2.5

Table 1. Water Quality

	2013 01-1	2013 01-3	2013 01-4	2013 01-5	2013 01-6	2013 01-	2013 01-	2013 01-1	2013 01-2	2013 01-4
	0.005	0.064	0.00	0.005	0.00	0.003	0.003	0.051	0.044	0.222
	0.021	0.34	0.044	0.042	0.02	0.031	0.033	0.310	0.25	1.450
	0.004	0.04	0.00	0.00	0.011	0.005	0.005	0.04	0.043	0.21
	0.011	0.232	0.036	0.044	0.012	0.034	0.00	0.123	0.00	0.3
	0.00	0.036	0.03	0.03	0.06	0.026	0.025	0.046	0.031	0.06
	0.26	1.10	6.600	1.0	0.3	0.233	1.150	1.50	0.516	0.15
	0.406	0.2	0.12	0.112	0.0	0.1	0.054	0.16	0.11	0.65
	0.046	0.034	0.014	0.02	0.050	0.030	0.010	0.050	0.02	0.130
	0.11	0.144	0.203	0.364	0.042	0.04	0.0	0.066	0.042	0.03
	2013 01-5	2013 01-6	2013 01- (1)	2013 01- (1)	2013 01- (1)	2013 03-2 (1)	2013 03-3 (1)	2013 03-4 (1)	2013 03-5 (1)	2013 01-3 (2)
	4.1	45.	4.	53.1	51.1	50.40	50.54	50.52	51.22	52.3
2	0.34	0.15	1.40	1.24	1.31	1.0	1.63	1.31	1.1	0.33
3	1.	1.5	16.5	16.1	15.3	15.	16.6	15.55	15.4	1.61
3	4.52	3.34	.	.11	.43	.0	.50	.42	.2	3.44
	0.0	0.0	0.11	0.10	0.11	0.13	0.11	0.14	0.12	0.0
	6.	.42	4.0	4.2	4.41	5.	3.2	6.06	.14	4.
	11.03	12.61	6.22	5.5	6.3	6.5	4.52	.4	.26	0
	4.6	.3	.2	.3	.00	4.52	.31	4.0	4.0	.11
	0.13	0.11	0.3	0.31	0.42	2.04	0.33	1.2	2.03	0.1
5	0.04	0.02	0.62	0.62	0.65	0.4	0.6	0.4	0.44	0.04
	3.2	3.26	4.24	2.54	2.3	2.2	5.14	2.65	1.3	2.
	.5	.2	.6	.0	.4	.40	.1	.6	.6	.1
	4.	.4	.11	.0	.42	6.56	.64	6.0	6.11	.2
#	5	1	55	54	54	56	41	56	64	4
	.	4.5	1.16	1.12	1.4	.	40.4	5.2	6.2	5.1
	0.22	0.135	1.24	1.63	1.316	1.53	1.034	1.100	0.55	0.62
	25.0	23.	1.6	1.5	1.5	.5	1.2	25.2	1.	1.0
	11	3.	1.6	166	1.2	22	22	254	1	5.
	34.	163	60.5	62.6	64.1	116	1.	0.	203	23.
	24.2	21.6	26.	23.6	24.6	2.	2.5	2.0	2.0	16.4
	4.	1.5	63.6	50.	51.4	6.	2.	5.3	132	1.1

Major elements (%)

Trace elements (ppm)



Table 1. $^{40}\text{Ar}/^{39}\text{Ar}$ ratios

	2013 年 01 月 5	2013 年 01 月 6	2013 年 01 月 (C 1)	2013 年 01 月 (C 1)	2013 年 01 月 (C 1)	2013 年 03 月 2	2013 年 03 月 3	2013 年 03 月 4	2013 年 03 月 5	2013 年 01 月 3
$^{40}\text{Ar}/^{39}\text{Ar}$	3.0	1.20	3.60	46.0	4.30	23.40	43.00	25.20	32.0	6.56

Table 1. (continued)

	2013, 01-11 (n = 2)	2013, 02-1 (n = 2)	2013, 02-2 (n = 2)	2013, 03-1 (n = 1)	2013, 03-6 (n = 1)	2013, 01-10 (n = 2)	04/06 (n = 1)	04/24 (n = 1)	04/2 (n = 1)	03/1 (n = 1)
<i>Trace elements (ppm)</i>										
	1.4	36.	42.4	26.0	32.4	1.	/	/	/	/
	0.35	0.153	0.35	1.1	0.4	0.46	/	/	/	/
	32.5	33.2	34.5	25.1	26.3	32.1	13.4	20.5	1.	20.3
	1.4	203	21	33	341	1.5	144	1.4	214	265
	56.5	44.2	4.	1.	22.2	53.	15	162	214	265
	34.	3.5	3.3	23.1	24.	33.	20.6	30.	2.	20.2
	66.4	4.6	6.4	25.4	2.1	66.6	.1	114	5.5	.02
	6.4	236.4	256.	205.4	20.	114.20	/	/	/	/
	4.0	44.1	4.0	4.	103	44.1	/	/	/	/
	12.0	11.1	11.2	14.	13.6	12.0	/	/	/	/
	0.5	1.420	1.00	3.130	3.20	0.53	4.	1.1	22.0	1.2
	1	1.50	5	2.0	24	6.6	.1	31	111	6
	13.0	13.0	13.2	21.1	22.	12.5	13.2	13.2	14.	20.1
	54.	42.3	41.5	144	154	52.	243	133	164	151
	1.2	0.4	0.55	11.315	11.5	1.25	20.2	12.	21.	12.2
	0.025	0.030	0.02	0.051	0.052	0.02	/	/	/	/
	0.31	0.26	0.32	1.560	1.450	0.360	/	/	/	/
	0.2	1.20	1.030	0.365	0.406	0.336	/	/	/	/
	11	3.2	346	25	50	4.3	/	/	/	/
	10.0	.40	.610	26.40	26.0	10.50	30.6	32.2	40.1	26.4
	23.00	1.0	1.40	51.50	54.0	22.30	5.	62.	2.3	52.5
	2.0	2.520	2.510	5.50	6.10	2.60	6.	.4	10.5	6.4
	11.0	11.0	11.60	22.30	24.30	11.60	2.5	31.2	43.1	24.4
	2.540	2.00	2.60	4.40	4.00	2.30	4.5	5.2	6.	4.5
	0.6	0.1	0.0	1.163	1.25	0.3	1.45	1.5	2.0	1.03
	2.40	2.13	2.54	4.14	4.46	2.522	3.56	4.01	5.35	4.23
	0.36	0.3	0.3	0.612	0.660	0.34	0.4	0.54	0.64	0.63
	2.10	2.150	2.220	3.420	3.60	2.130	2.5	2.	3.24	3.5
	0.46	0.446	0.444	0.2	0.5	0.46	0.4	0.52	0.5	0.
	1.350	1.230	1.240	2.120	2.20	1.310	1.32	1.3	1.45	2.25
	0.10	0.16	0.15	0.304	0.32	0.14	0.1	0.2	0.2	0.34
	1.210	1.050	1.120	1.60	2.110	1.210	1.25	1.23	1.24	2.13
	0.14	0.164	0.165	0.21	0.323	0.13	0.20	0.1	0.1	0.34
	1.30	0.41	1.040	3.20	3.510	1.460	5.3	3.2	4.16	3.2
	0.04	0.062	0.051	0.5	0.644	0.0	1.35	0.6	1.16	0.6
	0.151	2.0	1.50	2.5	1.	0.33	/	/	/	/
	0.34	0.206	0.200	45.20	35.10	0.41	.13	.0	4.1	21.06
	1.0	0.61	0.1	.60	.20	1.0	4.50	2.63	3.20	.41
	0.500	0.304	0.302	2.30	3.40	0.501	1.	0.6	1.46	2.5

04/06, 04/26, 04/2, 04/1 et al. (200 a).

Table 2. U-Pb zircon ages and geochemical data for the Zhaheba ophiolite. The first column lists the sample IDs, the second column shows the number of grains analyzed, and the following columns provide the $^{206}\text{Pb}/^{238}\text{U}$ and $^{207}\text{Pb}/^{235}\text{U}$ ratios, their uncertainties, and the resulting ages and MSWD values.

Sample	n	$^{206}\text{Pb}/^{238}\text{U}$	σ	Age (Ma)	$^{207}\text{Pb}/^{235}\text{U}$	σ	Age (Ma)	MSWD	$^{147}\text{Sm}/^{144}\text{Sm}$	$^{143}\text{Nd}/^{144}\text{Nd}$	σ	Age (Ma)	$^{143}\text{Nd}/^{144}\text{Nd}$	σ
2013-01-3	2	0.36	0.002	485.8	0.04030	0.002	485.8	3.1	2.4	0.134	0.004	485.8	0.5124	0.004
2013-01-10	2	0.5	0.0024	485.8	0.045	0.002	485.8	3.1	11.6	0.1235	0.004	485.8	0.5124	0.004
2013-03-1	1	3.13	0.0335	485.8	0.06324	0.003	485.8	3.1	4.4	0.121	0.004	485.8	0.5122	0.004
2013-03-2	1	2.1320	0.0063	485.8	0.042	0.002	485.8	3.1	4.5	0.1046	0.004	485.8	0.5124	0.004
2013-03-3	1	0.06	0.0452	485.8	0.0536	0.003	485.8	3.1	5.2	0.0	0.004	485.8	0.5124	0.004
2013-03-4	1	0.65	0.01	485.8	0.0422	0.002	485.8	3.1	4.55	0.1123	0.004	485.8	0.5125	0.004

$$t = 10000 \left(\frac{^{206}\text{Pb}/^{238}\text{U}}{^{207}\text{Pb}/^{235}\text{U}} \right) / (t - 1) \times 10^6 \text{ (Ma)}$$

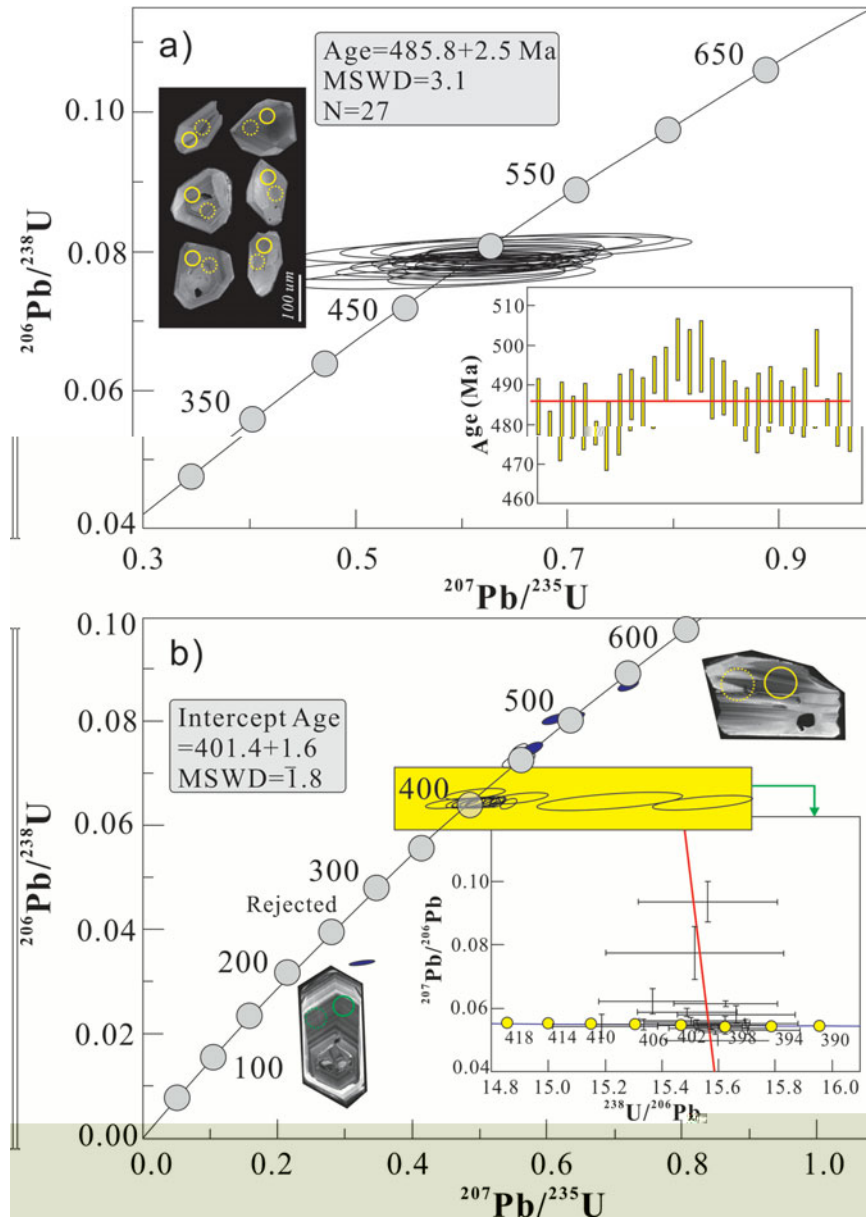
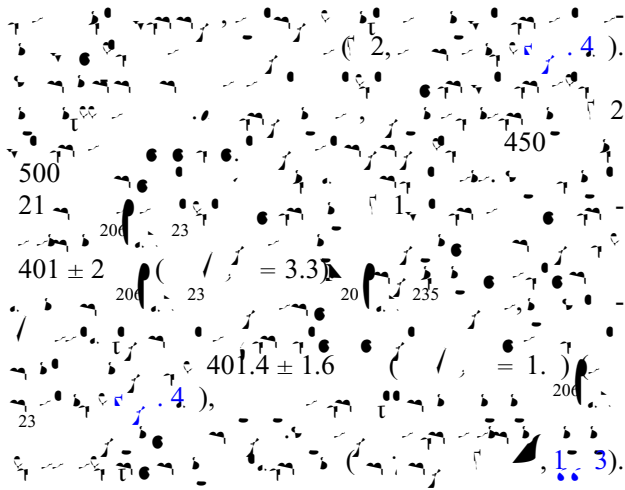
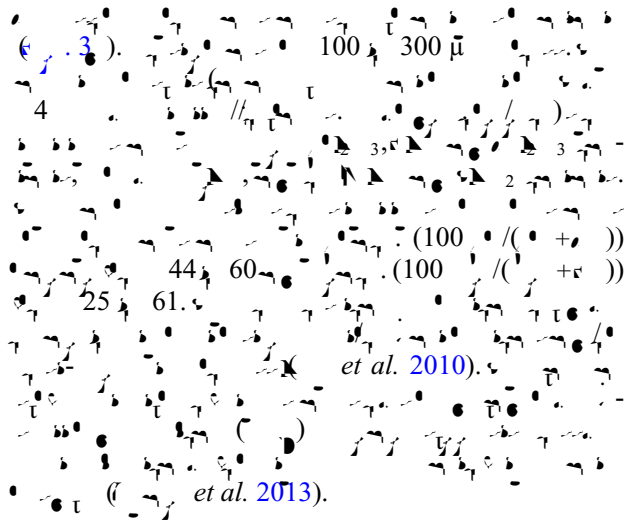


Table 3. U-Pb zircon ages and geochemical data for the Zhaheba ophiolite. The first column lists the sample IDs, the second column shows the number of grains analyzed, and the following columns provide the $^{206}\text{Pb}/^{238}\text{U}$ and $^{207}\text{Pb}/^{235}\text{U}$ ratios, their uncertainties, and the resulting ages and MSWD values.

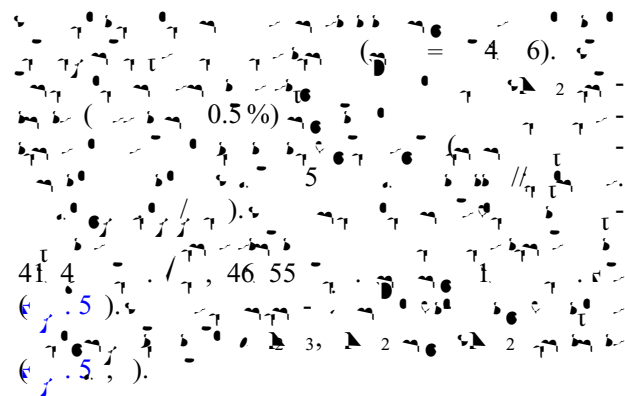
Figure 4. (a) $^{206}\text{Pb}/^{238}\text{U}$ vs. $^{207}\text{Pb}/^{235}\text{U}$ concordia diagram for sample 2013-01-3. The concordia line is defined by the equation $t = 10000 \left(\frac{^{206}\text{Pb}/^{238}\text{U}}{^{207}\text{Pb}/^{235}\text{U}} \right) / (t - 1) \times 10^6$ (Ma). The age is 485.8 ± 2.5 Ma, MSWD = 3.1, N = 27. (b) $^{206}\text{Pb}/^{238}\text{U}$ vs. $^{207}\text{Pb}/^{235}\text{U}$ concordia diagram for sample 2013-03-1. The intercept age is 401.4 ± 1.6 Ma, MSWD = 1.8. A shaded region indicates rejected data points. Inset shows age histogram with a mean age of 401.4 ± 1.6 Ma. Micrographs show zircon grains with analytical pits.



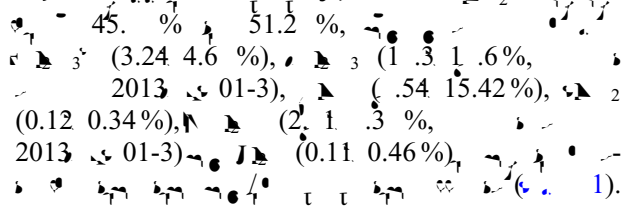
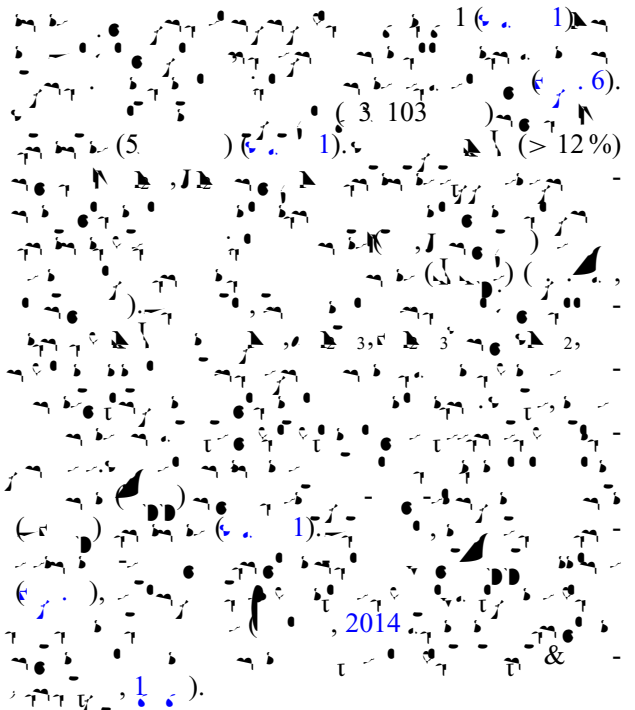
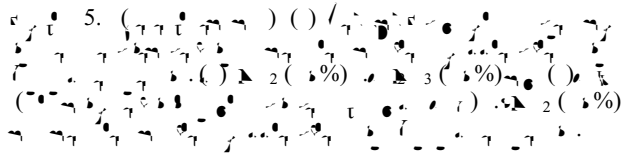
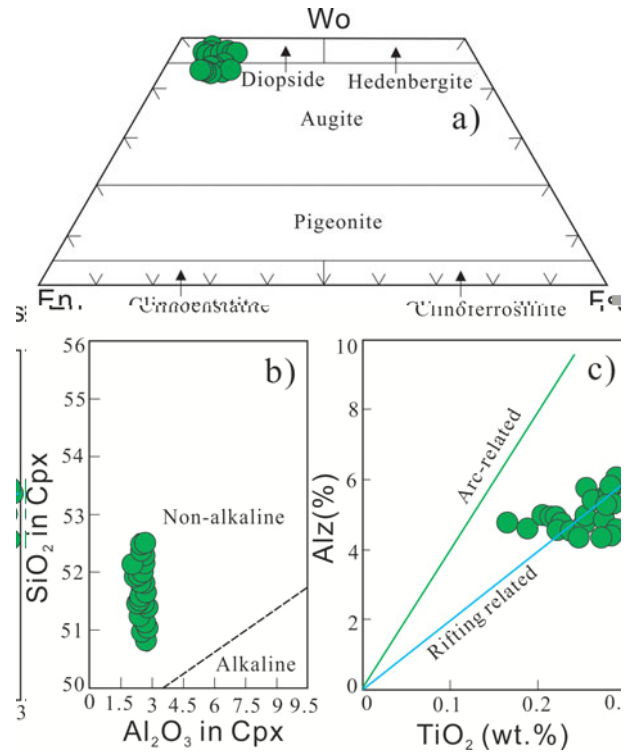
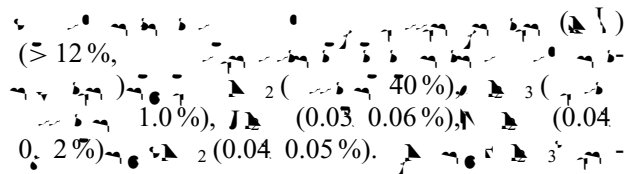
4.b. M a c
4.b.1. Spinel composition



4.b.2. Pyroxene compositions



4.c. W a c
4.c.1. Serpentinites and cumulates



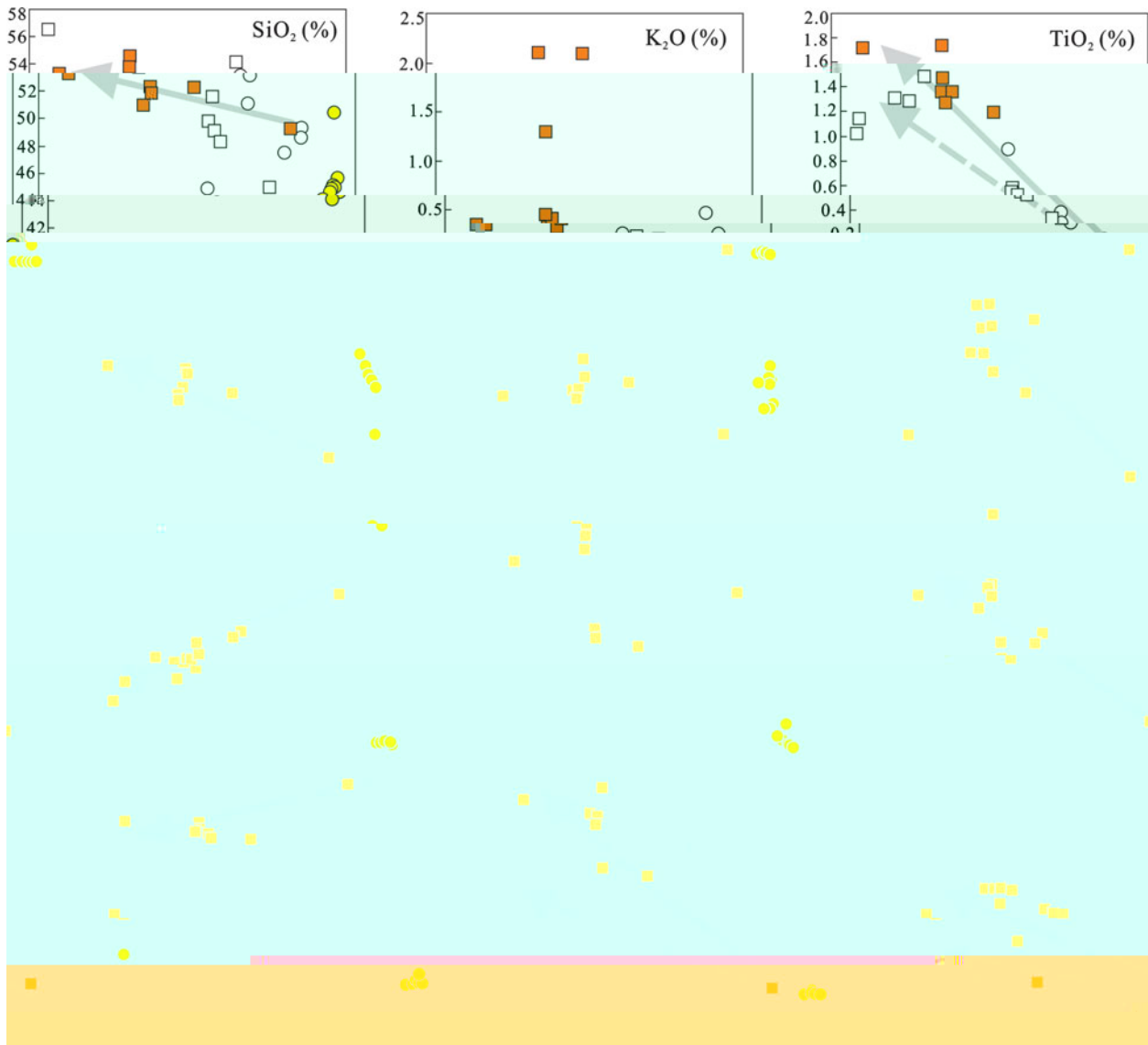


Figure 6. (a) Geochemical data for the Zhaheba ophiolite. (b) Map of the study area showing the distribution of the ophiolite units. (c) Map of the study area showing the distribution of the ophiolite units. *et al.* 2000 a

Figure 6. (a) Geochemical data for the Zhaheba ophiolite. (b) Map of the study area showing the distribution of the ophiolite units. (c) Map of the study area showing the distribution of the ophiolite units. *et al.* 2000 a

Figure 6. (a) Geochemical data for the Zhaheba ophiolite. (b) Map of the study area showing the distribution of the ophiolite units. (c) Map of the study area showing the distribution of the ophiolite units. *et al.* 2000 a

Figure 6. (a) Geochemical data for the Zhaheba ophiolite. (b) Map of the study area showing the distribution of the ophiolite units. (c) Map of the study area showing the distribution of the ophiolite units. *et al.* 2000 a

Figure 6. (a) Geochemical data for the Zhaheba ophiolite. (b) Map of the study area showing the distribution of the ophiolite units. (c) Map of the study area showing the distribution of the ophiolite units. *et al.* 2000 a

Figure 6. (a) Geochemical data for the Zhaheba ophiolite. (b) Map of the study area showing the distribution of the ophiolite units. (c) Map of the study area showing the distribution of the ophiolite units. *et al.* 2000 a

Figure 6. (a) Geochemical data for the Zhaheba ophiolite. (b) Map of the study area showing the distribution of the ophiolite units. (c) Map of the study area showing the distribution of the ophiolite units. *et al.* 2000 a

4.c.2. Basalts

Figure 6. (a) Geochemical data for the Zhaheba ophiolite. (b) Map of the study area showing the distribution of the ophiolite units. (c) Map of the study area showing the distribution of the ophiolite units. *et al.* 2000 a

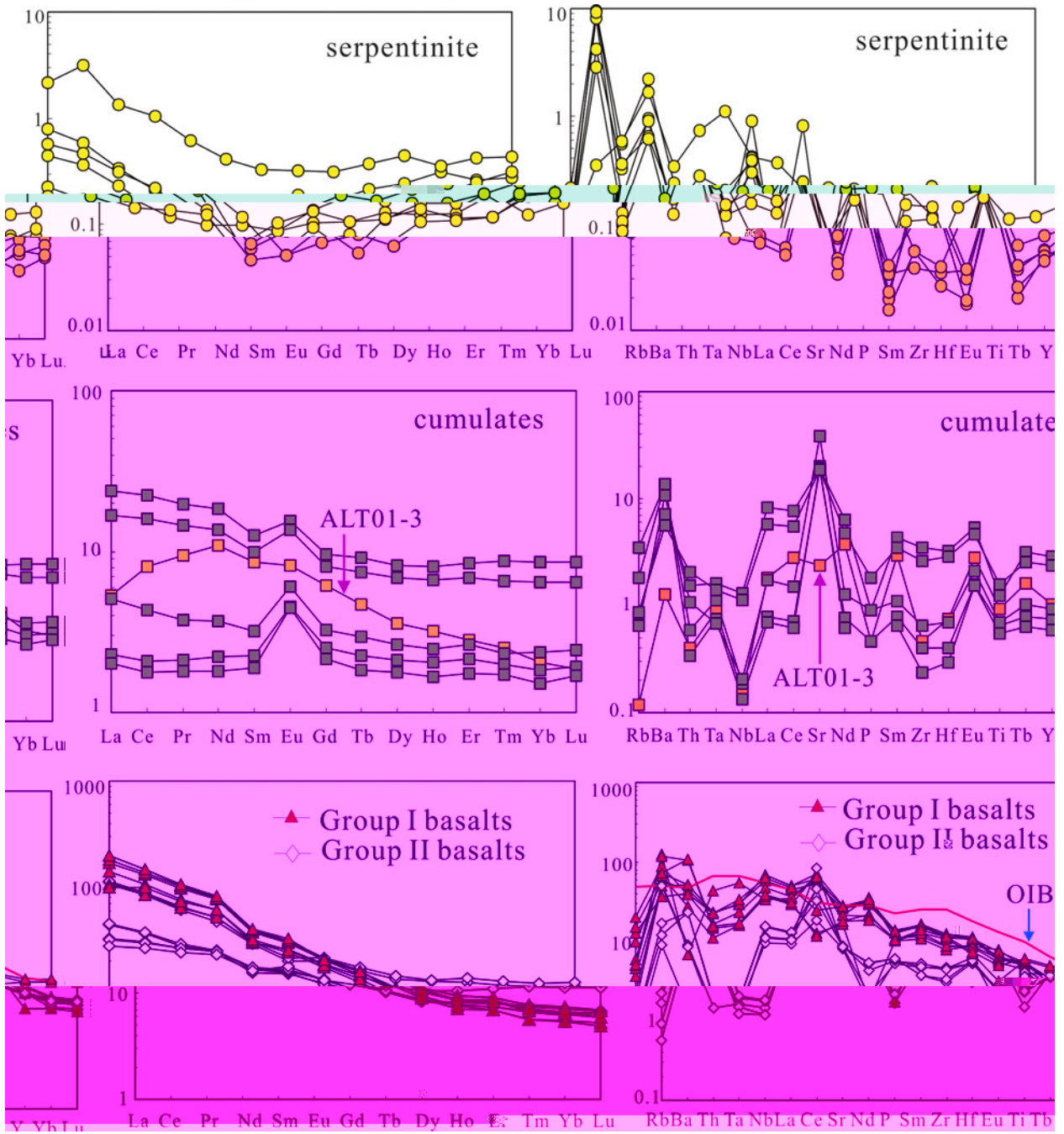


Figure 4. REE and trace element patterns for serpentinite, cumulates, and basalts. The OIB pattern is from the OIB array (see text for details).

$(\text{D}_T/\text{D}_U = 0.0 - 1.14)$
 $(\text{D}_T/\text{D}_U = 1.02 - 1.21)$
 $(\text{D}_T/\text{D}_U = 0.44)$
 (~ 0.11)

4. . W -pc S+Na z g H O
 2. 1.
 (0.0024 0.0452) / 6 (0. 04030
 0. 0536) / 6 (0. 04015 0. 05171,
 2013 03 1).
 0.0 0.13 4 143 /144
 0.512 0 0.512 3 (t)
 +6.3 + .5 (2013 03 1
 +1.).

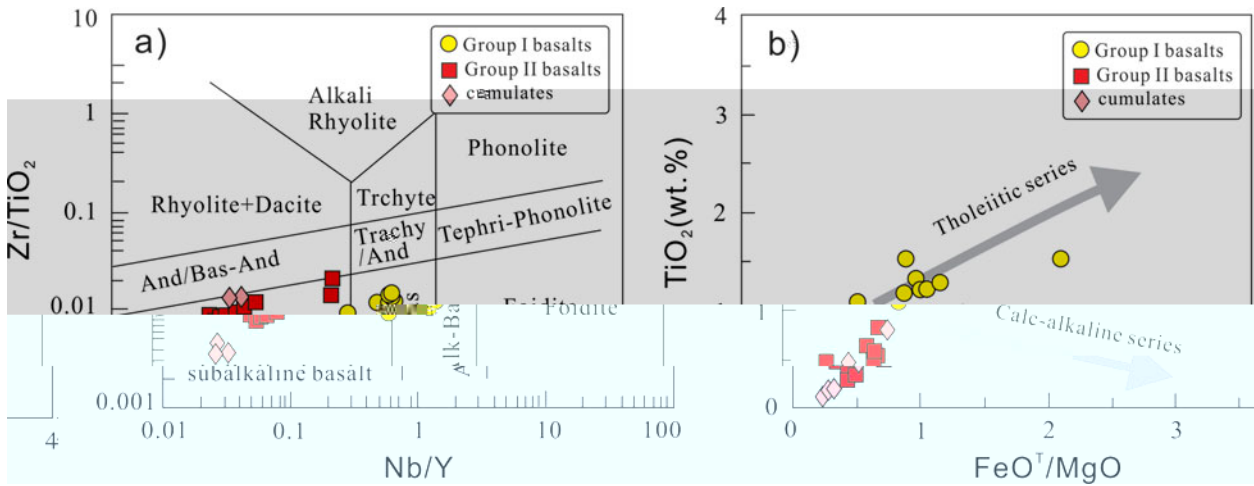


Figure 1. Geochemical diagrams for the Zhaheba ophiolite. (a) Zr/TiO₂ vs Nb/Y diagram showing various volcanic fields. (b) TiO₂ (wt.%) vs FeO^T/MgO diagram showing the Tholeiitic and Calc-alkaline series.

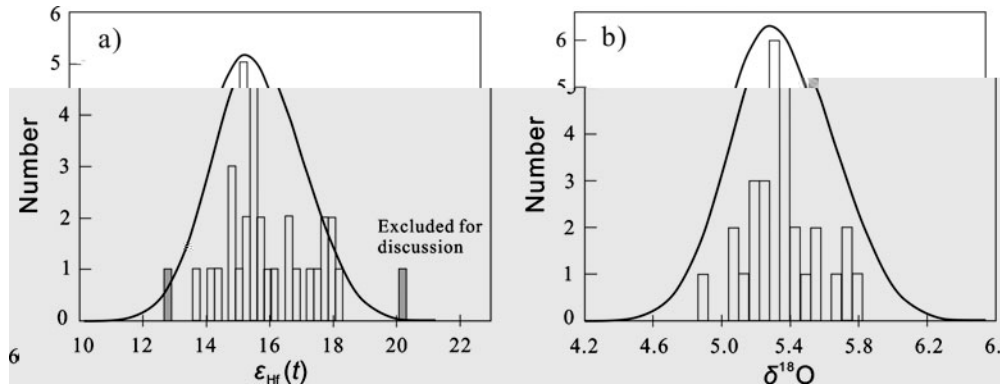


Figure 2. Histograms of $\epsilon_{Hf}(t)$ (a) and $\delta^{18}O$ (b) for the Zhaheba ophiolite.

(2013, 01) ... $\epsilon_{Hf}(t) > 16$... $\delta^{18}O$... $5.3 \pm 0.23\%$... $\epsilon_{Hf}(t)$... 1.4 ± 0.2 ... 6.0 ... 200 ... 200 ... $et al.$

5. D ... 5.a. T ... b ... Z a ba ... 401 ... $(503 \pm \dots)$... (416 ± 3) ... $et al.$... 2012 ... $et al.$... 200 ... b, s, \dots ... (401) ... (46) ... $1, 3$... (1) ... $et al.$

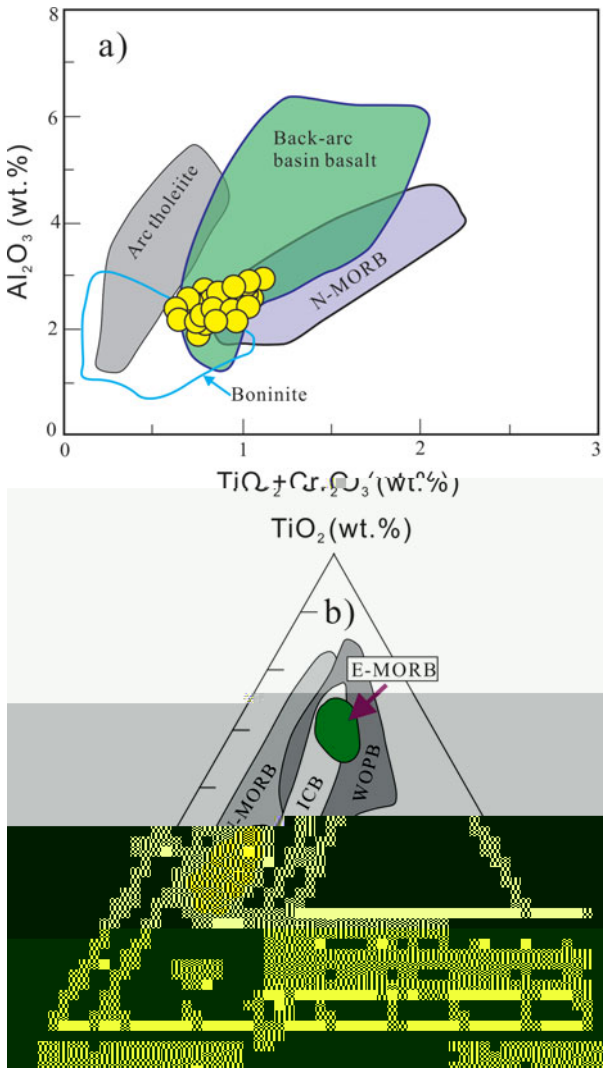


Fig. 11. (a) Al_2O_3 (wt.%) vs. $TiO_2 + Cr_2O_3$ (wt.%) diagram showing fields for Arc tholeiite, Back-arc basin basalt, N-MORB, and Boninite. (b) TiO_2 (wt.%) vs. $TiO_2 - Cr_2O_3$ (wt.%) diagram showing fields for MORB, ICB, WOPB, and E-MORB. A green oval highlights a specific data point in the E-MORB field.

(Fig. 12),

(Fig. 12),

et al. (2002)

(Fig. 12),

(Fig. 12),

5.c. P... D... a... b... r...

(11.24)

15... (0.4-0.6%)

(11.15, 60)

(Fig. 2)

2001 (Fig. 13)

(1)

2002) (2)

(Fig. 2) & et al. (Fig. 6)

(Fig. 2) & et al. (Fig. 6)

2001) (Fig. 2) & et al. (Fig. 6)

(0.0412-0.06133) (t)

(+1.5-1.5)

(3.44-20.4)

(1.5-2.54)

(Fig. 6)

(Fig. 1)

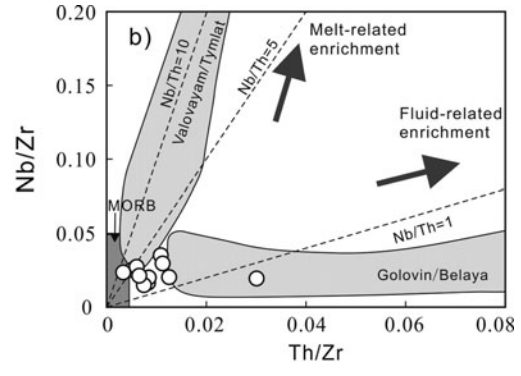
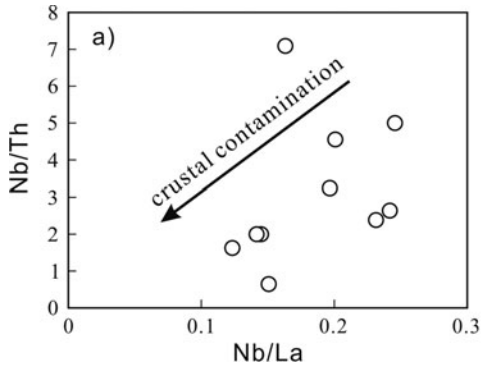
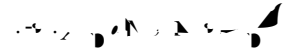
et al.

(Fig. 6) & et al. (Fig. 6)

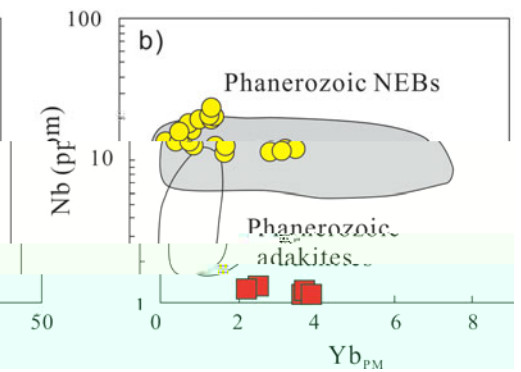
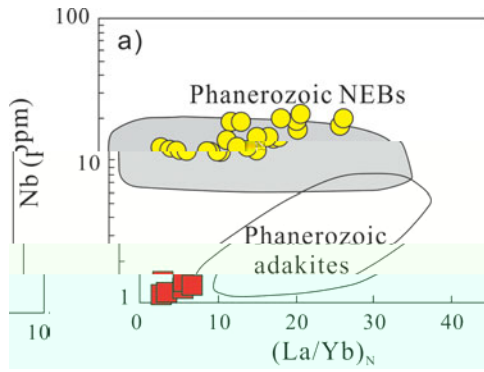
2000)

& et al. (Fig. 2) et al. (Fig. 6)

(200)



12. (Nb/Th) vs (Nb/La) and (Nb/Zr) vs (Th/Zr) diagrams. The arrow indicates crustal contamination. The fields represent MORB, Valovayami/Tymjal, Melt-related enrichment, Fluid-related enrichment, and Golovin/Belaya.

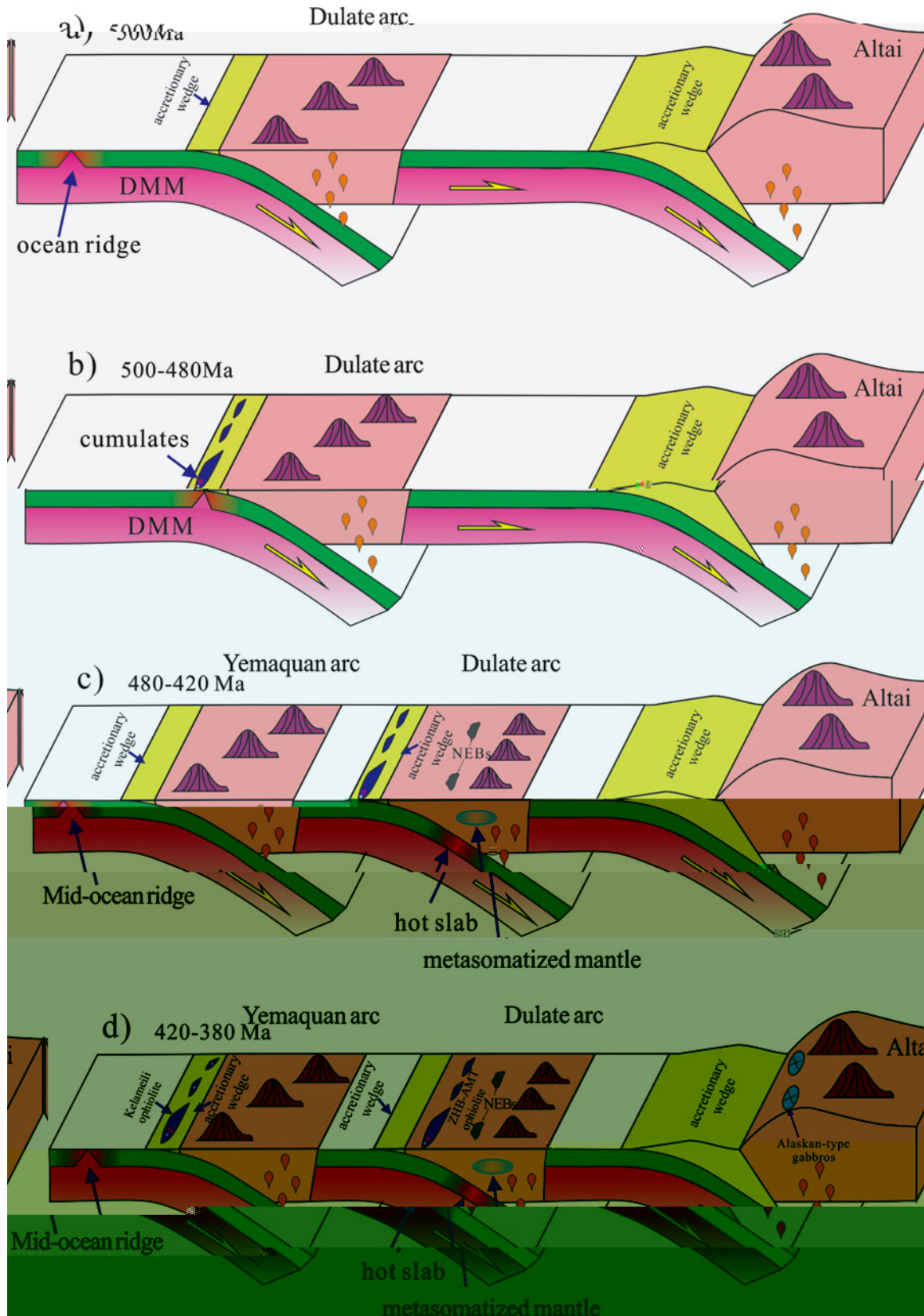


13. (Nb) vs ((La/Yb)N) and (Nb) vs (YbPM) diagrams. The shaded areas represent Phanerozoic NEBs and Phanerozoic adakites.

(t) (1.5) (76) (0.04120 0.06133)
(t) (/6)
2. (< 0.3) (/6)
& 1.1 (2002).
2. (0.1 0.2) (0.6 1.0)
& 1.6.
(14).

(14). 2.
2.

5. I ca Pa a z c acc c
a a
(416 et al. 2014
et al. 2015), (503
4 5 et al. 2003 et al. 2015)
(400) (1)
(et al. 2014),
et al. 200, 200 a,b et al.
200 a).
(et al. 200 b).



15. (a) 500 Ma, (b) 500-480 Ma, (c) 480-420 Ma, (d) 420-380 Ma. The diagram illustrates the tectonic evolution of the Dulate and Yemaquan arcs, showing the progression from an ocean ridge to a mid-ocean ridge, the formation of accretionary wedges, and the involvement of a hot slab and metasomatized mantle. Key geological features include the DMM (Dulate Mantle Melange), cumulates, NEBs (Nevada-Eurasian Basin), Kelameit ophiolite, ZHB-AMT ophiolite, and Alaskan-type gabbros.

(4) *et al.* 2014 *et al.* 2015). (420 3 0)
 1. 2.
 (15).
 (400 3 0).

6. C c

(1) 4 5 c.
 400
 (2)
 (3)

Ac

305
 (2011, 06 03-01).

S7 a a a

// /10.101 / 0016 56 16000042.

R / c
 1. 4.
Chemical Geology 113, 1 1 204.
 & . 2001.
Journal of Petrology 42, 22 302.
 & . 200
Lithos 97, 2 1
 2002 &
Geology 30, 10.
 & . 200
Earth Accretionary Systems in Space and Time (&), 1 36.
 & . 2002.
Geological Magazine 139, 1 13.
 3.
Geological Society of America Bulletin 105, 15 3
Ophiolites, 220
 & . 3.
Geology 21, 54 50.
 & . 2.
Journal of Geological Society, London 149, 56
 & . 4.
Contributions to Mineralogy and Petrology 86, 54 6.
 & / . 2003
 (2) *Ophiolites in Earth History* (&), 43 6
 21
 & . 2011
Geological Society of America Bulletin 123, 3 411.
 & . 2015.
Chinese Journal of Geology 50, 140 54
 & / . 2000.
 ()
Contributions to Mineralogy and Petrology 140, 2 3 5
 & . 1.
Lithos 27, 25

- Geological Bulletin of China 30, 150-153.
- & . 2011. *Geochimica et Cosmochimica Acta* 75, 504-512.
- . 2001. *Nature* 410, 6-11.
- & . 2002. *Chemical Geology* 182, 22-35.
- & . 1996. *Journal of Geophysical Research: Solid Earth* (1978-2012) 101, 11-31.
- & J. . 2000. *Contributions to Mineralogy and Petrology* 139, 20-26.
- & . 2012. *Geological Bulletin of China* 31, 126-131.
- & . 2014. *Chinese Science Bulletin (Chinese Version)* 59, 2213-2221.
- & . 2000. *Transactions of the Royal Society of Edinburgh: Earth Sciences* 91, 1-3.
- & . 2000. *Journal of Petrology* 31, 6-11.
- & . 2003. *Earth Science Frontier* 10, 43-56.
- J. & . 2001. *Journal of Petrology* 42, 655-671.
- J. . 1996. *Nature* 380, 23-40.
- & . 2000. *Tectonophysics* 326, 255-261.
- . 2010a. *Lithos* 114, 1-15.
- . 2004. *Geological Magazine* 141, 225-311.
- & . 2010b. *Geostandards and Geoanalytical Research* 34, 11-34.
- & . 2013. *Chinese Science Bulletin* 58, 464-474.
- & . 2000. *Lithos* 113, 2-4.
- & . 2010. *Chinese Science Bulletin* 55, 1535-1546.
- J. . 2003. *User's Manual for Isoplot 3.00: A Geochronological Toolkit for Microsoft Excel*. 4, 3-4.
- & . 2015. *Gondwana Research*, 10.1016/j.gr.2015.04.004.
- . 2015. *American Journal of Science* 274, 32-355.
- J. & . 1995. *Geology* 23, 51-54.
- . *Structure of Ophiolites and Dynamics of Oceanic Lithosphere*. 36-40.
- Journal of Petrology* 38, 104-114.
- J. . 2000 a. *Acta Petrologica Sinica* 25, 16-24.
- J. & . 2000 b. *Acta Petrologica Sinica* 25, 14-16.
- J. & . 2000. *Acta Petrologica Sinica* 23, 162-174.
- J. & . 2002. *Proceedings of the Ocean Drilling Program, Scientific Results, vol. 176* (1-60).

2000. *Chinese Science Bulletin* **14**, 216–21.
2010. *Lithos* **117**, 1–20.
2000. *Journal of Asian Earth Sciences* **30**, 666–5.
2000. *Lithos* **100**, 14–4.
2014. *Elements* **10**, 101.
2001. *Contribution to Mineralogy and Petrology* **141**, 36–52.
2013. *Gondwana Research* **24**, 3–2–411.
2006. *Journal of Petrology* **37**, 6–3–26.
2013. *Precambrian Research* **231**, 301–24.
2012. *Precambrian Research* **192–195**, 1–0–20.
2000. *Philosophical Transactions of the Royal Society of London* **335**, 3–2.
2000. *Nature* **377**, 5–5–600.
2000. *Nature* **364**, 2–3–30.
2014. *Lithos* **206–207**, 234–51.
2002. *Reviews of Geophysics* **40**, 3–1–3–3.
2000. *Science in China Series D – Earth Sciences* **52**, 1345–5.
2000. *Magmatism in the Ocean Basin* (), 52–4–42.
2000. *Chemical Geology* **247**, 352–3.
2000. *Acta Petrologica Sinica* **23**, 1–33–44.
2000. *Contributions to Mineralogy and Petrology* **133**, 1–11.
2006. *Journal of Geology* **114**, 35–51.
2000. *Lithos* **110**, 35–2.
2012. *Earth-Science Reviews* **113**, 303–41.
2000. *Chemical Geology* **20**, 325–43.
2002. *Journal of Geology* **110**, 1–3.
2006. *Geology in China* **33**, 4–6–6.
2014. *Geoscience Frontiers* **5**, 525–36.
2000. *Journal of Asian Earth Sciences* **32**, 102–1.
2013. *Gondwana Research* **23**, 1316–41.
2004. *Journal of Geological Society, London* **161**, 33–42.

200. a. *International Journal of Earth Sciences* **98**, 11, 21.
- J. F. & N. S. 200. b. *American Journal of Sciences* **309**, 221. 0.
1. 3. *Regional Geology of the Xinjiang Uygur Autonomous Region*. 2 145 ().
2015. & *Journal of Asian Earth Sciences* **113**, 5.
2012. & *Gondwana Research* **21**, 246-65.
200. & N. S. 200. *Chemical Geology* **242**, 22-3.
2006. *Acta Geologica Sinica* **80**, 254-63 ().
2003. & N. S. *Chinese Science Bulletin* **48**, 2231-5.
2013. & N. S. *Lithos* **179**, 263-4.
2012. & N. S. *Journal of Asian Earth Sciences* **52**, 11-33.
200. & N. S. *Acta Petrologica Sinica* **24**, 1054-5 ().
1. 6. *Annual Review of Earth and Planetary Sciences* **14**, 4-3-5-1.